

# Changes in Cerebral Blood Flow and Postsynaptic Muscarinic Cholinergic Activity in Rats with Bilateral Carotid Artery Ligation

Yasuomi Ouchi, Hideo Tsukada, Takeharu Kakiuchi, Shingo Nishiyama and Masami Futatsubashi  
Positron Medical Center, Hamamatsu Medical Center; and Central Research Laboratory, Hamamatsu Photonics K.K., Hamakita-City, Shizuoka, Japan

Changes in both regional cerebral blood flow (rCBF) and postsynaptic muscarinic cholinergic activity in the rat brain were investigated after ligation of the common carotid arteries (CCAs) bilaterally with  $^{15}\text{O}$ -labeled water ( $\text{H}_2^{15}\text{O}$ ) and [ $^{11}\text{C}$ ]N-methyl-4-piperidylbenzilate, a potent muscarinic receptor antagonist. **Methods:** PET was performed in the same Wistar rat, 7 days and 1 mo after the CCA ligation. Regional cerebral blood flow and the transfer coefficient  $k_3$ , the rate of binding of  $^{11}\text{C}$ -NMPB, were measured, based on the autoradiographic method and the graphical plotting analysis, respectively. **Results:** The levels of rCBF in the frontal cortex of the ligated group were significantly lower than those in the cerebellum and those in sham group, after 7 days and 1 mo postoperation. Although the level of  $k_3$  in the frontal cortex 7 days after operation was not altered, it decreased significantly after 1 mo in the ligated group. Neither cortical infarct nor cortical neuronal loss was observed histologically. **Conclusion:** Common carotid artery ligation in Wistar rats caused a prolonged cerebral hypoperfusion without degeneration of the cortical neurons and a later decline of postsynaptic cholinergic receptor activity. These findings suggest that the decline in the postsynaptic cholinergic activity that is associated with the prolonged reduction in the cerebral blood supply may reflect pathophysiology that is equivalent to the deterioration of cognitive function in patients with chronic cerebrovascular insufficiency.

**Key Words:** cerebral hypoperfusion; [carbon-11]N-methyl-4-piperidylbenzilate; carotid artery ligation; PET

**J Nucl Med 1998; 39:198-202**

Ligation of the common carotid arteries (CCAs) in rats is a widely used experimental approach to study mild brain ischemia (1,2). Severe ischemia in the brain is, on the other hand, induced by this ligation in connection with lowering blood pressure by withdrawal of blood or additional ligation of other major cerebral arteries (3,4). Pathological studies show that ligation of CCAs in Wistar rats causes rarefaction in the cerebral white matter but neither neuronal degeneration nor tissue necrosis in the cortex within 6 mo after the surgery (5). This model could be a good model to study pathophysiology in chronic cerebral hypoperfusion that is attributable to the development of cerebrovascular insufficiency in aged humans. It remains unclear if this model produces a long-term reduction of regional cerebral blood flow (rCBF). PET permits the exact time-course evaluation of changes in rCBF after vascular insults.

Metabolically, CCA ligation results in reductions of cerebral metabolic rate of glucose in the cortex, 7 days postoperation (2), and of presynaptic cholinergic activity in the acute phase (6). This metabolic depression in the cortex might be partly due to loss of excitatory input by deafferentation of presynaptic

cholinergic projection (7). The presynaptic cholinergic deafferentation by lesioning basal forebrain in rats did not affect the uptake of cholinergic ligands [ $^3\text{H}$ ]quinuclidinyl benzilate (8) and [ $^{11}\text{C}$ ]N-methyl-4-piperidylbenzilate ( $^{11}\text{C}$ -NMPB) in our preliminary study (data not shown). Thus, it may not be possible to discuss the relationship between rCBF reduction and postsynaptic cholinergic activity in the brain.

This study re-evaluated changes in the brain perfusional state in the same rats, 7 days and 1 mo after ligation of bilateral CCAs, using PET and tested the hypothesis that loss of acetylcholine precursors in acute cerebral hypoperfusion is followed by reduction in postsynaptic radioligand uptake by measuring the rate of binding ( $k_3$ ) of  $^{11}\text{C}$ -NMPB, a muscarinic receptor antagonist (9).

## MATERIALS AND METHODS

### Materials

Twelve male Wistar rats, weighing 200–350 g, were studied. These rats were arbitrarily divided into two groups: ligated group ( $n = 6$ ) and sham group ( $n = 6$ ).

### Surgery

Under anesthesia (300 mg/kg chloral hydrate, injected intraperitoneally), bilateral CCAs, carefully separated from the vagosympathetic trunks, were exposed through a midline cervical incision and then doubly ligated with silk sutures. After ligation, rats were kept unrestrained in their home cages with food and water ad libitum. In the sham group, bilateral CCAs were loosely encircled with sutures.

### Magnetic Resonance Imaging Procedure

MRI (0.3 T MRP7000AD; Hitachi, Tokyo, Japan) was performed to superimpose PET images on MRI for selecting image slices and brain areas (Fig. 1) (10). Briefly, the acquisition parameters were as follows: three-dimensional mode sampling, TR/TE (200/23), 45° flip angle, 2-mm slice thickness with no gap and 256 × 256 matrices. Under anesthesia (400 mg/kg/hr chloral hydrate, intraperitoneally), rats were fixed in a stereotaxic acrylic head-holder with a marking site in ear bars filled with gadolinium-diethylenetriamine pentaacetic acid. The data were analyzed by the image processing system (Dr. View; Asahi Kasei Co., Tokyo, Japan) on a SUN workstation (Hypersparc ss-20; SUN Microsystems, CA). Registration proceeded with reference to three markers (a frontal pole of the forebrain and bilateral points of ear bars that had been marked in advance). This procedure eliminates the ambiguity of anatomical localization in small animals such as rodents when setting regions of interest (ROIs) on PET images.

### PET Procedure

A high-resolution PET scanner for animal use (SHR-2000; Hamamatsu Photonics K.K., Hamakita, Japan), equipped with four detector rings and producing seven-slice imaging (14 imagings possible with z-motion), was used. The spatial resolution at the

Received Oct. 15, 1996; revision accepted Mar. 19, 1997.

For correspondence or reprints contact: Yasuomi Ouchi, MD, PhD, Positron Medical Center, Hamamatsu Medical Center, 5000, Hirakuchi, Hamakita-City, Shizuoka 434, Japan.

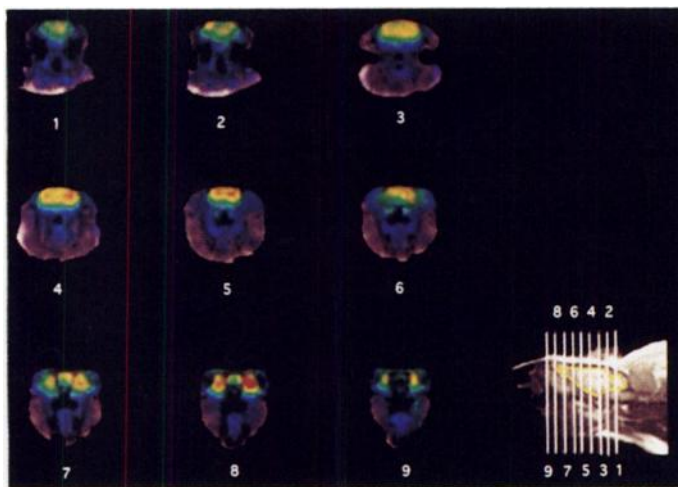


**FIGURE 1.** Rat  $^{11}\text{C}$ -NMPB PET images superimposed on MRIs. The numbers under the images correspond to the slice numbers drawn on the sagittal MRI image. As shown in Figure 2 image 1 was chosen as an image for the cerebellum ROI, image 4 was chosen for the caudate-putamen ROI and image 6 was chosen for the frontal cortex ROI. This superimposition technique clarified the extracranial activity from the periorbital gland observed in Images 7–9.

center was 3 mm horizontally and 4.8 mm axially at FWHM. Averaged direct slice sensitivity and the cross-slice sensitivity were 2.3 kcps/ $\mu\text{Ci}/\text{ml}$  and 3.8 kcps/ $\mu\text{Ci}/\text{ml}$ , respectively (11).

After MRI measurement, all rats were treated with arterial and venous catheterization under chloral hydrate anesthesia and with tracheotomy so that they could breathe the room air spontaneously. Before imaging, rats were placed in the prone position in the PET camera under continuous intravenous infusion of chloral hydrate (100 mg/kg/hr) through a cannula in the tail vein. The head of the rat was fixed horizontally with the same acrylic head-holder used for MRI and positioned with the aid of a laser beam. A 20-min transmission scan using  $^{68}\text{Ge}/^{68}\text{Ga}$  was performed for attenuation correction. After the transmission scan, we injected 148 MBq  $\text{H}_2^{15}\text{O}$  in bolus, and arterial blood samples were collected every 4 or 5 sec. Simultaneously, 10-sec PET scans of 12 consecutive frames were cumulatively obtained (12,13). Waiting for the decay of  $^{15}\text{O}$ , 37 MBq  $^{11}\text{C}$ -NMPB were injected intravenously with simultaneous measurement of sequential 32 PET scans: first, 16 frames at 1 min/scan and, then, the next 16 frames at 3 min/scan. No blood samples were obtained in the  $^{11}\text{C}$ -NMPB study. During PET examination, systemic arterial blood pressure and rectal temperature were continuously monitored, and arterial blood gases were measured periodically. These values were kept within physiological limits as follows: blood pressure, 96–110 mmHg;  $\text{PaCO}_2$ , 36.7–40.4 mmHg;  $\text{PaO}_2$ , 86–92 mmHg; pH, 7.38–7.42; and temperature, 37°C.

#### Data Analysis

As shown in Figure 2, the elliptical ROIs, ranging from 38–60  $\text{mm}^2$  were placed bilaterally on the frontal cortex and the caudate-putamen and one was placed symmetrically on the whole cerebellum. Figure 2 demonstrates that the ROI on the frontal cortex can include the subcortical white matter. As the rats were immobilized during  $\text{H}_2^{15}\text{O}$  and  $^{11}\text{C}$ -NMPB studies, we could obtain two types of brain time-activity curves for these two radioisotopes in the same ROI. Measurement of rCBF was based on the autoradiographic method (12–14). All 12 frames were used for further analysis. The values for both partition coefficient and extraction fraction of  $\text{H}_2^{15}\text{O}$  were fixed at 1. As shown in a human study with  $^{11}\text{C}$ -NMPB (15), quantitative evaluation of the binding rate ( $k_3$ ) of  $^{11}\text{C}$ -NMPB was made by applying the graphical plotting method, which required no blood sampling and originated from the previous

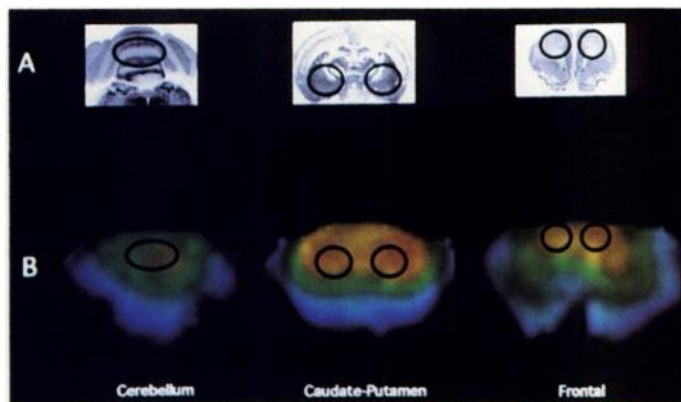


**FIGURE 2.** ROI setting. (A) Histological images from a rat brain atlas (32). (B) Elliptical and circular ROIs, ranging from 38 to 60  $\text{mm}^2$ , are drawn on the cerebellum, caudate-putamen and frontal cortex.

studies (16–18). Cholinergic terminals from the basal forebrain are rich in the frontal cortex (19), whereas the cerebellum contains few muscarinic cholinergic receptors (20). This allows use of the cerebellum as an inert region. The scattergram in Figure 3 plots radioactivities of a specific binding site (frontal cortex) (15), and the increments of the curves in the frontal cortex demonstrate that the rate of dissociation ( $k_4$ ) of the ligand was negligible and that it bound irreversibly during the experiment. The conclusive equation of the plotting method is expressed as:  $M_s(t)/M_{ns}(t) = k_3 * \int M_{ns}(u)du/M_{ns}(t) + V$ , where  $M_s(t)$  and  $M_{ns}(t)$  denote the specific binding region (frontal cortex) and the nonspecific binding region (cerebellum), respectively. In this equation,  $k_3$  was determined as the slope of the straight line obtained by plotting  $M_s(t)/M_{ns}(t)$  ratio against the normalized integral,  $\int M_{ns}(u)du/M_{ns}(t)$  (15,18). The values of rCBF and  $k_3$  in the frontal cortex and caudate-putamen were determined by the average of bilateral values.

#### Statistics

The values of rCBF and  $k_3$  at 7 days postoperation were compared separately between two groups using one-way analysis

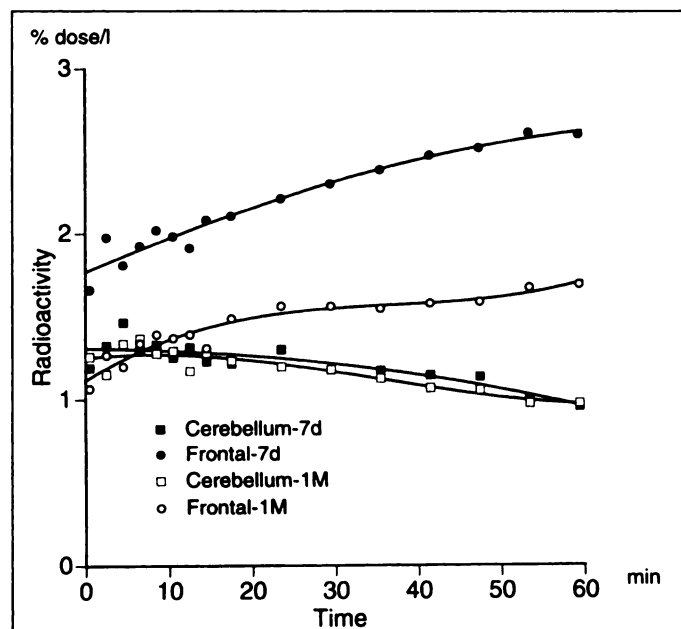


**FIGURE 3.** Time course of  $^{11}\text{C}$ -NMPB accumulation in the frontal cortex (specific binding) and cerebellum of the ligated rat. The curve of the frontal cortex was obtained by subtracting counts in cerebellum from the measured counts in the frontal cortex. This scattergram shows that the accumulation in the frontal cortex was lower at 1 mo than it was at 7 days postoperation ( $p < 0.001$ ), without any significant difference in radioactivity in the cerebellum.

TABLE 1

Results of Regional Cerebral Blood Flow and  $k_3$  for Carbon-11-N-Methyl-4-Piperidylbenzilate in the Common Carotid Artery—Ligated and Sham Groups

Group	Area	rCBF (ml/100 g/min)		$k_3$ (min <sup>-1</sup> )	
		7 days	1 mo	7 days	1 mo
CCA	Frontal	47.9 ± 4.1*	44.6 ± 4.9*	0.0192 ± 0.0029	0.0075 ± 0.0008†
	Caudate-putamen	54.8 ± 3.9*	50.8 ± 9.2*	0.0175 ± 0.0036	0.0095 ± 0.0014†
	Cerebellum	86.4 ± 8.8	83.3 ± 10.6		
Sham	Frontal	65.0 ± 4.1	75.4 ± 12.1	0.0168 ± 0.0033	0.0182 ± 0.0011
	Caudate-putamen	67.7 ± 3.3	74.1 ± 4.2	0.0155 ± 0.0035	0.0167 ± 0.0011
	Cerebellum	78.6 ± 4.7	75.4 ± 12.1		

Values are expressed as mean ± s.d.

\* $p < 0.01$  compared to sham group.

† $p < 0.001$  compared to 7-day values of CCA group, and  $p < 0.0001$  compared to sham group.

of variance (ANOVA) with post hoc Scheffe's F-test. These parameters, at 1 mo postoperation, also were analyzed using the same test procedures. The time courses of differences in rCBF and  $k_3$  between the two groups were examined by repeated ANOVA with post hoc Scheffe's F-test. Statistical significance was assumed at  $p$  values less than 0.05.

### Histology

Brains were removed from all animals after the 1-mo PET examination to examine the occurrence of vascular insult using cresyl violet staining.

### RESULTS

The  $H_2^{15}O$  study showed that rCBF values in the frontal cortex and caudate-putamen in the ligated group remained significantly lower than those in the sham group, at 7 days ( $p < 0.001$ ) and 1 mo ( $p < 0.003$ ) after the operation. Repeated ANOVA disclosed no significant differences in rCBF levels of the frontal cortex and the caudate-putamen between 7 days and 1 mo postoperation (Table 1 and Fig. 4).

The  $^{11}C$ -NMPB study showed that there was no reduction in  $k_3$  in the frontal cortex and the caudate-putamen 7 days after the operation, whereas a significant reduction in  $k_3$  was observed in those areas 1 mo after the operation, compared with the sham group ( $p < 0.0001$ ). Repeated ANOVA also showed the significant decline of  $k_3$  value in the ligated group ( $p < 0.001$ ) (Table 1 and Fig. 5).

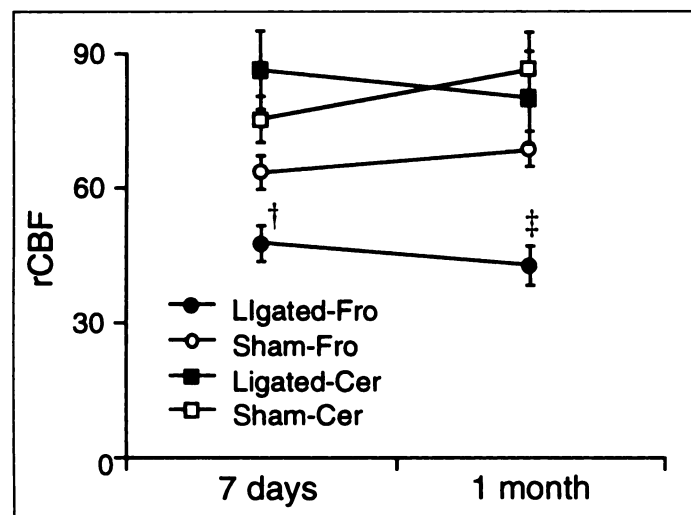


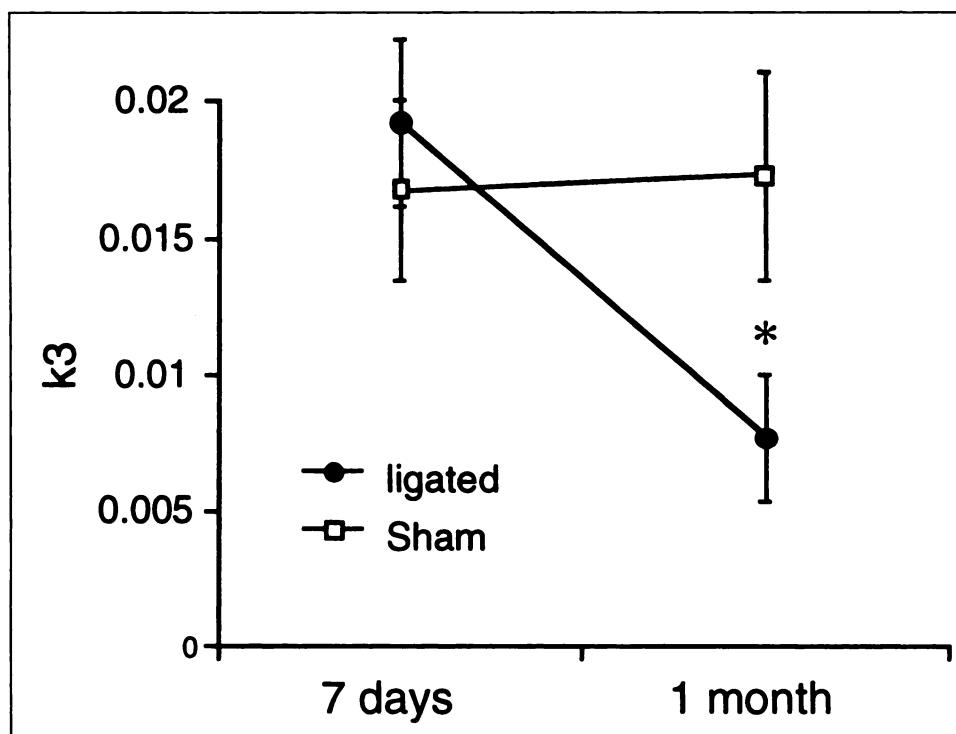
FIGURE 4. Change in rCBF. There is a consistent low perfusion in the frontal cortex of the ligated group. Fro = frontal cortex; Cer = cerebellum; † = significant difference between ligated and sham group at 7 days; ‡ = significant difference between ligated and sham group at 1 mo.

Figure 3 shows an example of the time course of changes in  $^{11}C$ -NMPB radioactivity in the frontal cortex and cerebellum of the ligated group. One month after the operation, the accumulation of  $^{11}C$ -NMPB was reduced in the frontal cortex, whereas the cerebellar radioactivity remained unchanged. Microscopic examination using cresyl violet staining showed no cortical necrosis in any of the operated rats in this study (Fig. 6).

### DISCUSSION

This study has several limitations. Although we used superimposition techniques, it was impossible to achieve the precise fitting of ROIs between the 7-day and 1-mo data in the concerned area. The use of morphological information might reduce the ROI positioning error as minimally as possible compared to previous studies in which the rat atlas was used. Second, there may be the problem of partial volume effect caused by small-sized ROIs. To minimize this effect, we made the ROI size larger than 2 FWHM (21). The final problem is the effect of anesthesia, which can change metabolism and CBF in vivo. Although the electroencephalogram was not monitored, the physiological data remained stable during measurements.

An animal model of chronic cerebral hypoperfusion was produced by ligating bilateral CCAs of rats (1,2) in connection with hampering the blood stream from the unilateral subclavian artery (3). These autoradiographic studies showed significant rCBF reduction in the infarction-free frontal cortex after 1–3 wk (22), and cortical glucose consumption was reduced after 7 days postoperation (2). This study demonstrated that ligating bilateral CCAs of Wistar rats resulted in prolonged hypoperfusion in the neocortex without causing cortical infarction and later decline in postsynaptic cholinergic receptor activity. Our results support that such ligation in a Wistar rat can be a means to establish chronic cerebral hypoperfusion. Different results in glucose metabolism and postsynaptic cholinergic activity in the cortex 7 days after operation is of interest. The reduction of cerebral metabolic rate of glucose measured with [ $^{14}C$ ]deoxyglucose may reflect decreased presynaptic functions including cholinergic system. Because  $^{11}C$ -NMPB is a compound for evaluating postsynaptic cholinergic function, it may be that the postsynaptic receptor activity is enhanced compensationally or resultantly by functional or structural alterations of the cholinergic receptors at a comparatively early stage of cerebral low perfusion. Presynaptically, acute brain ischemia altered the concentrations of the precursors for acetylcholine synthesis: acetyl-CoA, originating from pyruvate, and choline, from hydrolysis of phospholipids (6). However, loss of cholinergic input from the basal forebrain in an acute lesion model did not affect postsynaptic activity studied with [ $^3H$ ]quinuclidinyl ben-



**FIGURE 5.** Changes in  $k_3$  in the frontal cortex. Repeated ANOVA shows significant reduction in  $k_3$  in the ligated group 1 mo after the operation (\*).

zilate (8) and with  $^{11}\text{C}$ -NMPB in our preliminary study (data not shown). Thus, it is plausible that increased occupancy of the receptors by acetylcholine released in a compensatory manner under such acute ischemia may raise the substantial radioligand uptake. The determination of the  $B_{\text{max}}$  and the frequent measurements of the receptor activities would be of value.

A previous study showed that early decreased glucose metabolism in the frontal cortex was normalized 3 wk after suppression of presynaptic cholinergic system (7). It is unlikely that the presynaptic cholinergic damage is solely responsible for deactivation of the postsynaptic receptor activity in the prolonged low perfusional state. Pharmacologically, acetylcholine regulates postsynaptic neuronal activities through intracellular signaling processes (23,24). Postsynaptic excitation normally increases the energy requirement and enhances the regional metabolic rates of glucose and oxygen and rCBF (25). Therefore, it is possible that excessive or tonic release of acetylcho-

line results in down-regulation of receptor activities, shown as the later decline of radioligand uptake in this study, and that prolonged inadequate blood supply would diminish the energy metabolism in postsynaptic neurons and cause severe enough structural loss of receptors (e.g., loss of dendrites) to reduce the ligand binding.

Carbon-11-NMPB is, indeed, a potent muscarinic cholinergic antagonist and exhibits high brain extraction, but it is a non-subtype-selective agent (9). Thus, this ligand is not appropriate for evaluating pathological conditions, which are characterized as changes in subtypes (m1–m5) of muscarinic cholinergic receptors. Because the dissociation rate of  $^{11}\text{C}$ -NMPB is not completely negligible, the graphical plotting method applied here for quantification of  $k_3$  might be inappropriate, and dynamic method with arterial blood sampling using three-compartment, four-parameter analysis might have been useful instead, as shown previously (7). However, because this study showed no alterations in rCBF of the cerebellum, which was selected as a reference region, it was acceptable to compare the magnitudes of  $k_3$  obtained by the graphical plotting method between groups. The reduction of  $k_3$  may have been attributed to the reduction in influx rate,  $K_1$ , of  $^{11}\text{C}$ -NMPB, related to a decrease in rCBF, but this is unlikely for the following reasons. First, there were no alterations in  $k_3$  value at 7 days postoperation when rCBF was significantly reduced. Second, a previous simulation study of the effects of altered blood flow on the kinetics of thalamus/occipital cortex indicated that  $k_3$  was little affected because the binding rate is much smaller than the rates of transport across the blood-brain barrier (26).

Cerebrovascular insufficiency is characterized by cerebral blood flow that is inadequate to fulfill the brain metabolic needs. Under such conditions, spatial memory acquisition and retention in rats (27,28) and humans (29–31) have been shown to be progressively impaired. Although no precise behavioral tests were performed in this study, it did seem that the behavioral responses of the ligated rats when they were seized by hands or stimulated with flashlight were a little slow

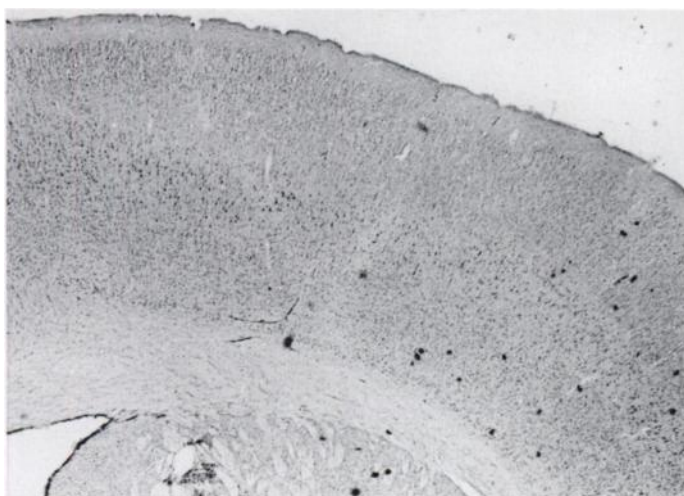


**FIGURE 6.** Microscopic appearance of cresyl violet staining of the cerebral cortex in ligated rats after the second PET, showing no incidence of cortical infarction or neuronal degeneration.

compared with sham-operated rats 1 mo after the operation. These cognitobehavioral findings present the possibility that the decline of the pre- and postsynaptic cholinergic system under prolonged cerebral hypoperfusion may contribute to the etiology of developing dementia.

## CONCLUSION

A Wistar rat with ligated bilateral CCAs served as a model to prolong cerebral hypoperfusion. Decline in the postsynaptic cholinergic activity, which is associated with such prolonged inadequate cerebral blood supply, may be related to the pathophysiology of chronic cerebrovascular insufficiency in humans.

## ACKNOWLEDGMENTS

We thank Hiroyuki Okada, Etsuji Yoshikawa and Shuji Nobezawa for technical support.

## REFERENCES

1. Eklof B, Siesjo BK. The effect of bilateral carotid artery ligation upon the blood flow and the energy state of the rat brain. *Acta Physiol Scand* 1972;86:155-165.
2. Tsuchiya T, Sako K, Yura S, Yonemasu Y. Local cerebral glucose utilization following acute and chronic bilateral carotid artery ligation in Wistar rats: relation to changes in local cerebral blood flow. *Exp Brain Res* 1993;95:1-7.
3. de la Torre JC, Fortin T, Park GAS, et al. Chronic cerebrovascular insufficiency induces dementia-like deficits in aged rats. *Brain Res* 1992;582:186-195.
4. de la Torre JC, Park AS, Fortin T, et al. Alzheimer-like deficits after chronic brain ischemia in rats [Abstract]. *Ann Neurol* 1991;30:286.
5. Wakita H, Tomimoto H, Akiguchi I, Kimura J. Glial activation and white matter changes in the rat brain induced by chronic cerebral hypoperfusion: an immunohistochemical study. *Acta Neuropathol* 1994;87:484-492.
6. Scremin OU, Jenden DJ. Time-dependent changes in cerebral choline and acetylcholine induced by transient global ischemia in rats. *Stroke* 1991;22:643-647.
7. Ouchi Y, Fukuyama H, Ogawa M, et al. Cholinergic projection from the basal forebrain and cerebral glucose metabolism in rats: a dynamic PET study. *J Cereb Blood Flow Metab* 1996;16:34-41.
8. Young AB, Frey KA, Agranoff BW. Receptor assays: in vitro and in vivo. In: Phelps ME, Mazziotta JC, Schelbert HR, eds. *Receptor assays: in vitro and in vivo*. New York, NY: Raven Press; 1986:82-83.
9. Mulholland GK, Kilbourn MR, Sherman P, et al. Synthesis, in vivo biodistribution and dosimetry of [<sup>11</sup>C]N-methylpiperidyl benzilate ([<sup>11</sup>C]NMPB), a muscarinic acetylcholine receptor antagonist. *Nucl Med Biol* 1995;22:13-17.
10. Ouchi Y, Okada H, Kakiuchi T, et al. Co-registration between PET and MRI in rat brain [Abstract]. *Ann Nucl Med* 1996;10(suppl):S143.
11. Watanabe M, Uchida H, Okada H, et al. A high resolution PET for animal studies. *IEEE Trans Med Imaging* 1992;11:577-580.
12. Magata Y, Saji H, Choi SR, et al. Noninvasive measurement of cerebral blood flow and

glucose metabolic rate in the rat with high-resolution animal positron emission tomography (PET): a novel in vivo approach for assessing drug action in the brains of small animals. *Biol Pharm Bull* 1995;18:753-756.

13. Ogawa M, Fukuyama H, Ouchi Y, et al. Uncoupling between cortical glucose metabolism and blood flow after ibotenate lesion of the rat basal forebrain: a PET study. *Neurosci Lett* 1996;204:193-196.
14. Herscovitch P, Markham J, Raichle ME. Brain blood flow measured with intravenous H<sub>2</sub><sup>15</sup>O. I. Theory and error analysis. *J Nucl Med* 1983;24:782-789.
15. Suhara T, Inoue O, Kobayashi K, Satoh T, Tateno Y. An acute effect of triazolam on muscarinic cholinergic receptor binding in the human brain measured by positron emission tomography. *Psychopharmacology* 1994;113:311-317.
16. Wong DF, Wagner HN Jr, Dannals RF, et al. Effects of age on dopamine and serotonin receptors measured by positron tomography in the living human brain. *Science* 1984;226:1393-1396.
17. Patlak CS, Blasberg RG. Graphical evaluation of blood-brain transfer constants from multiple-time uptake data. *J Cereb Blood Flow Metab* 1985;5:584-590.
18. Wong DF, Gjedde A, Wagner HN. Quantification of neuroreceptors in the living human brain. I. Irreversible binding of ligands. *J Cereb Blood Flow Metab* 1986;6:137-146.
19. Saper CB. Organization of cerebral cortical afferent systems in the rat. II. Magnocellularis basal nucleus. *J Comp Neurol* 1984;222:313-342.
20. Lin SC, Olson KC, Okazaki H, Richelson E. Studies on muscarinic binding site in human brain identified with [<sup>3</sup>H]pirenzepine. *J Neurochem* 1986;46:274-279.
21. Baron JC, Miyazawa, H. Use of positron emission tomography to assess effects of brain lesions in experimental subhuman primates. In: Michaelconn P, ed. *Methods of neurosciences: lesions and transplantation*. San Diego, CA: Academic Press; 1991: 429-441.
22. Mabe H, Uemura S, Iwayama K, Takagi T, Nagai H. Cerebral blood flow, EEG power spectrum and histopathology in experimental cerebral ischemia. *J Cereb Blood Flow Metab* 1981;1(suppl):S241-S242.
23. Brown JH, Brown SL. Agonists differentiate muscarinic receptors that inhibit cyclic AMP formation from those that stimulate phosphoinositide metabolism. *J Biol Chem* 1984;259:3777-3781.
24. Dauphin F, Lacombe P, Sercombe R, Hamel E, Seylaz J. Hypercapnia and stimulation of the substantia innominata increase rat frontal cortical blood flow by different cholinergic mechanisms. *Brain Res* 1991;553:75-83.
25. Roland PE. *Brain activation*. New York, NY: Wiley-Liss; 1993:501-504.
26. Frost JJ, Douglass H, Mayberg HS, et al. Multicompartment analysis of [<sup>11</sup>C]-carfentanil binding to opiate receptors in human brain measured by positron emission tomography. *J Cereb Blood Flow* 1989;9:398-404.
27. de la Torre J, Fortin T. A chronic physiological rat model of dementia. *Behav Brain Res* 1994;63:35-40.
28. Fieschi C. Cerebral blood flow and energy metabolism in vascular insufficiency. *Stroke* 1980;11:431-432.
29. Hagberg B, Ingvar DH. Cognitive reduction in pre-senile dementia related to regional abnormalities of cerebral blood flow. *Br J Psychiatry* 1976;128:209-222.
30. Lassen NA, Ingvar DH. Blood flow studies in the aging normal brain and in senile dementia. *Aging* 1980;13:91-98.
31. Lechner H, Niederkorn K, Schmidt R. Does cerebrovascular insufficiency contribute to Alzheimer's disease? *Ann NY Acad Sci* 1991;640:74-79.
32. Paxinos G, Watson C. *The rat brain in stereotaxic coordinates*. New York, NY: Academic Press; 1986.